

# Application of Finite-Volume Coastal Ocean Model in Studying Strong Tidal Currents in Discovery Passage, British Columbia, Canada

Yuehua Lin<sup>1</sup>, Jianhua Jiang<sup>1</sup>, David B. Fissel<sup>1</sup>, Michael G. Foreman<sup>2</sup>, Peter G. Willis<sup>1</sup>

## Abstract

The unstructured-grid, Finite-Volume Coastal Ocean Model (FVCOM) was used to simulate the flows in Discovery Passage, British Columbia, Canada. Challenges in this numerical study include the strong tidal currents in Seymour Narrows of up to  $7.8 \text{ m s}^{-1}$ , small-scale topographic features, and freshwater discharge and stratification. Tidal forcing, freshwater input, the Coriolis effect, and wet and dry regions were considered. The model was integrated for 16 days and model results of the last 14 days were examined. The model was validated using available historical measurements at different sites in Discovery Passage, including water surface elevation and ocean current data, as well as CTD-bottle profile data. Model results are also compared with the recent numerical studies by Jiang and Fissel (2007) and by Foreman et al. (2012). Model results demonstrated that the unstructured-grid model generated reasonable maps of the very strong currents in tidal channels, with the advantage of high adaptability in resolving the complex geometry of the narrow channels as seen in Discovery Passage. Effects of stratification and freshwater discharge from Campbell River during the study period were investigated.

## 1. Introduction

Discovery Passage (Figure 1) is a channel between Vancouver Island and Quadra Island (part of the Discovery Islands) off the British Columbia coast, connecting Johnstone Strait to the north and the Georgia Strait to the south. It is about 40 km in length and typically 2 km in width. The Campbell River is the major freshwater source in Discovery Passage located in the southern part of the channel on the eastern shore of Vancouver Island. During the last decades, large river discharge events can bring over  $850 \text{ m}^3\text{s}^{-1}$  of freshwater into the channel (Environment Canada's Hydrometric Database, HYDAT), normally occurring in winter due to seasonal rains.

---

<sup>1</sup>ASL Environmental Sciences Inc., #1-6703 Rajpur Place, Victoria, BC, V8M 1Z5, Canada, alin@aslenv.com, jjiang@aslenv.com, dfissel@aslenv.com, and pwillis@aslenv.com

<sup>2</sup>Institute of Ocean Sciences, Fisheries and Oceans Canada, Sidney, BC, V8L 4B2, Canada

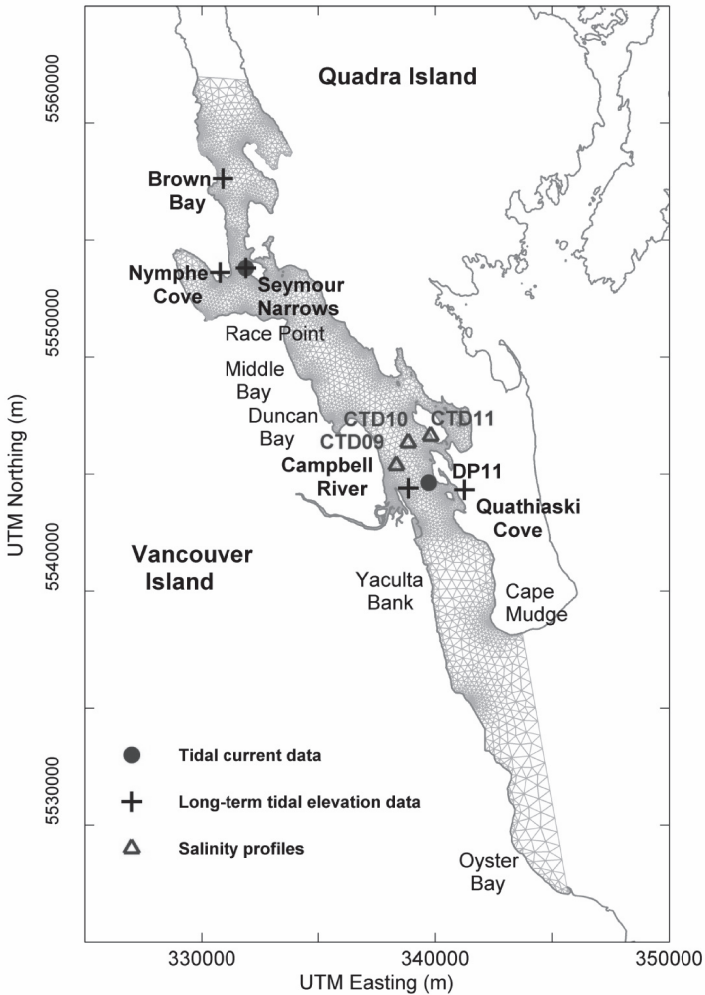


**Figure 1:** Map showing study area, model grids, and data sites. Positional data are presented in Universal Transverse Mercator (UTM) coordinates as UTM easting values, UTM northing values.

Discovery Passage is divided into two parts, Northern and Southern, by Seymour Narrows. Seymour Narrows is ~5 kilometer long, mostly ~750 meters wide, and nominally ~100 meters deep, known for strong tidal currents (up to  $7.8 \text{ m s}^{-1}$  based on Canadian Hydrographic Service, CHS, Canadian Tide and Current Tables) driven by a sea level difference of up to ~3 meters at the two ends of Discovery Passage (i.e., the Johnstone Strait and the Georgia Strait). Flood and ebb tides in Discovery Passage are associated with southward and northward flows. Strong tidal currents and small length scale in Seymour Narrows develop significant turbulence and consequent eddy diffusion and mixing. Discovery Passage is the preferred shipping route entering or leaving the Georgia Strait from the north. Moreover, the significant renewable tidal power potential in this area is drawing more and more interest from researchers, especially for numerical studies (e.g., Fissel et al., 2008; Jiang and Fissel, 2007, 2010; Sutherland et al., 2007).

Numerical modeling simulations of the currents and water levels in Discovery Passage were successfully conducted using the high resolution structured-grid three-dimensional, COastal CIRculation numerical Model (COCIRM), to assess the potential sites of installing and operating underwater turbines to generate electrical power (Fissel et al., 2008; Jiang and Fissel, 2007, 2010). However, it is the restraint from the conventional finite difference grid systems of COCIRM that leads us to carry out this numerical study using the unstructured-grid, Finite-Volume Coastal Ocean Model (FVCOM, version 3.1.4) developed by Chen et al. (2003, 2006a,b). FVCOM was used by Foreman et al. (2012) for studying the complex network of narrow channels and deep fiords in the Discovery Islands region, including Discovery Passage. We use their model results and available observations to assess our model performance in the model validation section. Employing a variable resolution triangular grid in FVCOM allows much more flexibility than a regular rectangular grid in representing complicated regions. This approach can provide high resolution for the coastline and the complicated geometry in Discovery Passage, while minimizing computer resources. In our study, the FVCOM model was run under Message Passing Interface (MPI) with 1 Linux computer (node) with 4 CPUs, each CPU containing 12 cores, totaling 48 CPU cores. All processes were run local to the single node.

This paper reports the model approaches and results in detail. Section 2 describes the model approach for the study. Section 3 presents the model validation for the control run. Section 4 discusses the influence of stratification and freshwater discharge on currents and volume transports in Discovery Passage, followed by summary and conclusion.

## 2. Model approach

The triangular grid for this FVCOM application has 6600 nodes with 11305 elements (Figure 1). The horizontal grid resolution varies from approximately 10 m for small islands to ~600 m in the middle channel. In the vertical, a sigma-coordinate system was applied with 12 levels. Higher resolution was used near both the surface

and the bottom and lower resolution was used at mid-column, with inter-layer spacing ranging from 0.014 to 0.153 of total water depth. The grid was generated with Gmsh (version 2.5) developed by Geuzaine and Remacle. The model bathymetry was generated from digitized nautical charts obtained from CHS (Chart No. 3539 and 3540). The bathymetric data were then interpolated onto the model grid and the depth contours are shown in Figure 2. Depth values are bottom elevation below chart datum (reduced to Lowest Normal Tide). The maximum water depth is up to 200 m in middle channel near the Brown Bay. The wetting-and-drying option was activated and the minimum water depth for a cell to be active was set to 1.0 m in FVCOM although it plays a minor role in overall circulation dynamics (Foreman et al., 2012).

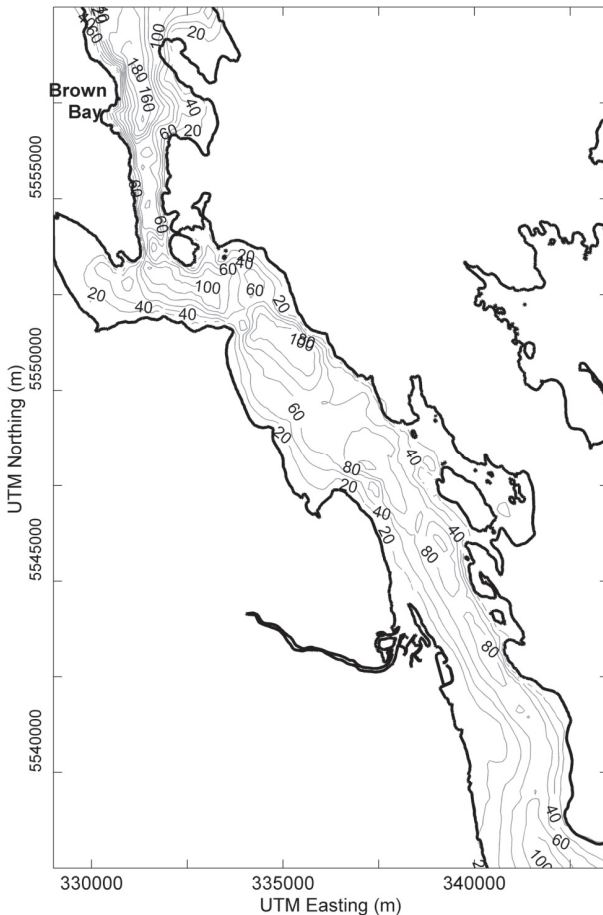


**Figure 2:** Major topographic features in the study area. Gray contours are bathymetry (unit: meter).

North	S2	M2	N2	K1	P1	O1	...
Amplitude(cm)	30.98	94.16	20.34	68.10	20.78	38.35	
Phase(Deg)	79.54	65.20	40.79	143.75	142.83	132.31	
South	S2	M2	N2	K1	P1	O1	...
Amplitude(cm)	21.73	85.45	18.25	88.40	27.68	51.10	
Phase(Deg)	172.44	154.72	131.19	166.70	164.33	155.15	

**Table 1:** Amplitudes and phases of few major tidal constituents in total 69 tidal constituents used in the model at open boundaries.

The FVCOM model employed a numerical integration with a second-order accurate finite volume flux discrete scheme, where internal and external modes are 'split' and integrated over distinct time steps. The external time step was determined to be 0.1 s (same as in Foreman et al., 2012) to preserve stability over the simulation. The ratio of time steps between the internal and external modes was set to 5 in this application. The Smagorinsky eddy parameterization (Smagorinsky, 1963) was used for horizontal diffusivity with coefficient  $C=0.2$ . The background vertical diffusion and viscosity were set to  $10^{-6} \text{ m}^2\text{s}^{-1}$  with a MY2.5 (Mellor and Yamada, 1982) turbulence closure. The bottom roughness parameter was set to 0.001 m with a minimal value of 0.005 for the model bottom drag coefficient.

The model was driven by tidal forcing at open boundaries and freshwater input from Campbell River. Surface winds were assumed to have little contribution to circulation during the study period (Foreman et al., 2012). The Coriolis effect was considered in the model. There are two open boundaries in the model where water surface elevations and inflow salinity and temperature were specified, i.e., at the north to Brown Bay and at the southern cross-section between Oyster Bay and Cape Mudge (Figure 1). Because of the dominant tidal flow in the channel and the absence of observational data, the model was driven with tidal elevations reconstructed from 69 tidal constituents at each open boundary. Those tidal constituents at open boundaries were extrapolated based on tidal height constituents inside the channel at Brown Bay, Nympe Cove, and Campbell River, where 1 – 2 year tidal elevations were used in the tidal analysis (Jiang and Fissel, 2007). Table 1 shows the amplitude and phase of major tidal constituents used in the model at open boundaries. For example, M2 has amplitude of around 0.9 m. The amplitude and phase difference between the northern and southern open boundaries for M2 are about 0.1 m and  $90^\circ$ . Tidal elevation time series at open boundaries during the study period were then derived from those tidal height constituents using Foreman's tidal prediction program (Foreman, 1977). Tidal elevations were assumed to be uniform over the cross-sections of both open boundaries due to the absence of observational data.

As an extension of previous studies (Fissel et al., 2008; Jiang and Fissel, 2007, 2010) and considering the availability of historical observations to validate the model, the model was integrated for 16 days from August 26 to September 10 in 1968. Model results were saved for every half hour. Freshwater discharge applied in the model at Campbell River was retrieved from daily discharge reported in the Canadian Hydrological Data (HYDAT). The river discharge ranged from about 35 to 90  $\text{m}^3\text{s}^{-1}$  during the study period (Figure 3), which is relatively small compared with the maximum 580  $\text{m}^3\text{s}^{-1}$  during winter time in 1968. Model results of the last 14 days were examined and presented in this study based on two numerical experiments: the baroclinic control run and a barotropic run.

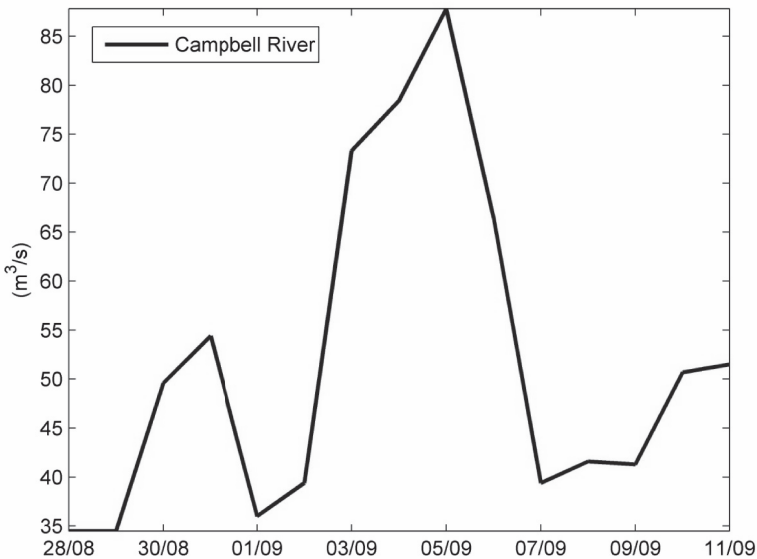


**Figure 3:** Campbell River discharges during the study period between August 28 and September 10 in 1968.

#### (1) Control Run (CR)

The initial salinities and temperatures over the whole model domain and inflow salinities and temperatures at open boundaries were specified based on the monthly salinity and temperature profile data near the southern boundary (Figure 4) reported in Crean and Ages (1971). The explicit Orlanski radiation (Orlanski, 1976; Chapman, 1985) boundary condition was used for salinities and temperatures. Due to the absence of daily or higher frequency variations, inflow salinities and temperatures along the boundaries were nudged back to the initial state with a timescale of 1 day. Considering the fact that water temperature fields play a minor role compared with water salinity fields in the study area (Fissel et al., 2010; Jiang and Fissel, 2007,

2010), only the tracer equation for salinity was activated in the simulation. The river discharge was assigned zero salinity (i.e. freshwater).

The model was validated using available historical measurements at different sites in Discovery Passage, including CHS water surface elevation, and IOS (Institute of Ocean Sciences) ocean current data from Department of Fisheries and Oceans (DFO) Canada, as well as CTD-bottle profile data at sites across the channel north of Campbell River (IOS). Model results were also compared with the recent numerical study by Jiang and Fissel (2007) which covered a similar model domain using the COCIRM model.

## (2) Barotropic Run (BT)

To investigate the baroclinic effect associated with stratification and freshwater discharge from Campbell River, a barotropic run was carried out with uniform and constant salinities and temperatures in the model. In this case the model was forced by the same tidal elevations at two open boundaries and the same volume transport input from Campbell River. The model salinities and temperatures were initialized and specified with a constant value all the time throughout the study area and there is no tracer equation involved.

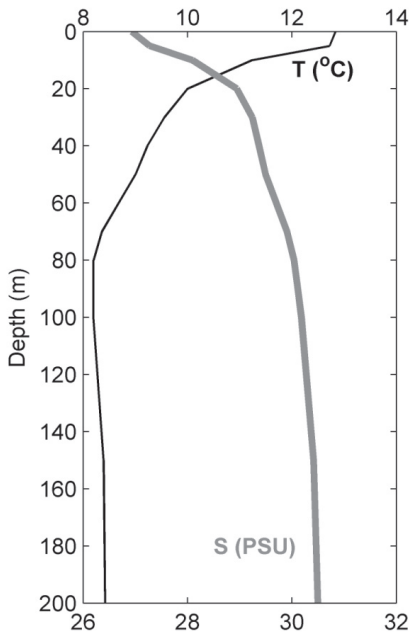


**Figure 4:** The vertical distributions of initial fields and inflow salinities (thick gray line) and temperatures (thin black line) at open boundaries.

### 3. Model validation for the control run

In this section the model performance is assessed by comparing model results with available observations and other numerical studies in Discovery Passage. Water levels, currents, and salinities values were saved for every half hour. The pattern of time-mean surface circulation and water levels produced by the model (Figure 5) are comparable with previous numerical results from Foreman et al. (2012). In the region of Seymour Narrows, associated with high speed currents, there is a water-head reduction.

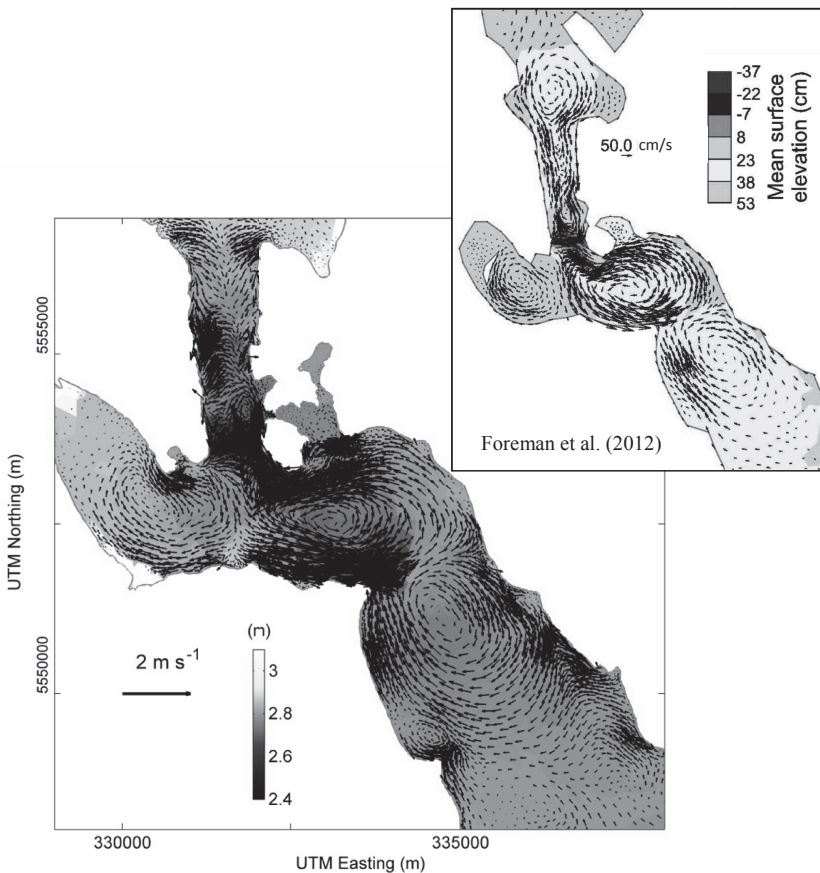


**Figure 5:** Model time-mean flows at 1m depth and surface elevations during the study period between August 28 and September 10 in 1968. Model results during the period of April 4-28 in 2010 from Foreman et al. (2010) are shown for comparison.

Hence the time-mean water levels are ~1.5 meter lower than in other areas. As to flow features, at about 5552500 m UTM Northing (Universal Transverse Mercator), a well-developed clockwise eddy and a well-developed counterclockwise eddy appeared during the study period at the southern entrance to Seymour Narrows, associated with the strong inflow and outflow there. In Middle Bay (around 335000 m UTM Easting and 5515000 m UTM Northing), due to the effect of the headland feature of Race Point, a well-defined clockwise eddy developed during the study period. The model results are very similar to the previous high resolution model study by Jiang and Fissel (2007 and 2010). Compared with Foreman et al. (2012) also using FVCOM, more details were resolved in this higher resolution model such as the small counterclockwise eddy at the south coastal region in Middle Bay. However, it should be noted that there is a discrepancy in the surface flow pattern between the control run and Foreman et al. (2012) in the region of northwestern Seymour Narrows. The vertical current profiles were not well reproduced in Foreman et al. (2012) at both moorings further north in Discovery Passage and south of Cape Mudge. In general, the model in Foreman et al. (2012) covers much larger area but captured less coastal and bathymetric details in the Discovery Passage, which they are planning to improve by refining their grid resolution.

The model results were compared with hourly tidal prediction reconstructed from 69 tidal constituents. Those tidal constituents were achieved based on 1 – 2 year measurements of water levels or currents at each site, and predicted tidal elevations were derived from those tidal height constituents using Foreman's tidal prediction program (Foreman, 1977) and used for model validation. Water surface levels produced by the model were compared with predicted tidal elevations (PTE) at Brown Bay, Seymour Narrows, Campbell River, Nympe Cove, and Quathiaski Cove as marked in Figure 1. Model generated currents were compared with predicted tidal currents (PTC) at different depths at Seymour Narrows and DP11 (as marked in Figure 1).

As seen in the comparisons (Figure 6) for water levels, model results appear to be in very good agreement with tidal predictions over the entire 14 day study period, including low frequency variations. The associated root-mean-square deviation (RMSD) between model produced water levels and the PTE is listed in Table 2. Typical flood and ebb flows at the surface are shown in Figure 7. Results are comparable with the previous numerical study by Jiang and Fissel (2007). Flood currents in Discovery Passage flow southward through the channel and ebb currents flow northward. Overall flow patterns in this area correspond to the bathymetric features of the channel. For example, in Middle Bay, flows are strongly affected by the prominent protrusion of Race Point (Figure 1) into the channel. During the ebb tide, the flow was separated at the eastern side of Race Point and water squeezed into Seymour Narrows. During the flood tide, the strong outflow from Seymour Narrows hit the coast of Vancouver Island and was separated at the northern side of Race Point.

Model generated current speeds and directions at the sites of Seymour Narrows (at 1 m depth) and DP11 (at 10 m and 22 m depths separately) were compared with tidal current prediction results based on observed currents and tide analysis (Jiang and Fissel, 2007) in Figure 8. The RMSD for eastward and northward components (U and V) between model produced and the PTC is shown in Table 3 individually. Given the strong currents, it is shown in Figure 8 that the model reasonably reproduced the tidal flow speeds and directions in Seymour Narrows. However, there were only slight discrepancies between model and tidal prediction currents at middle depth (22 m) at the DP11 site, with some over-predicted speed peak values.

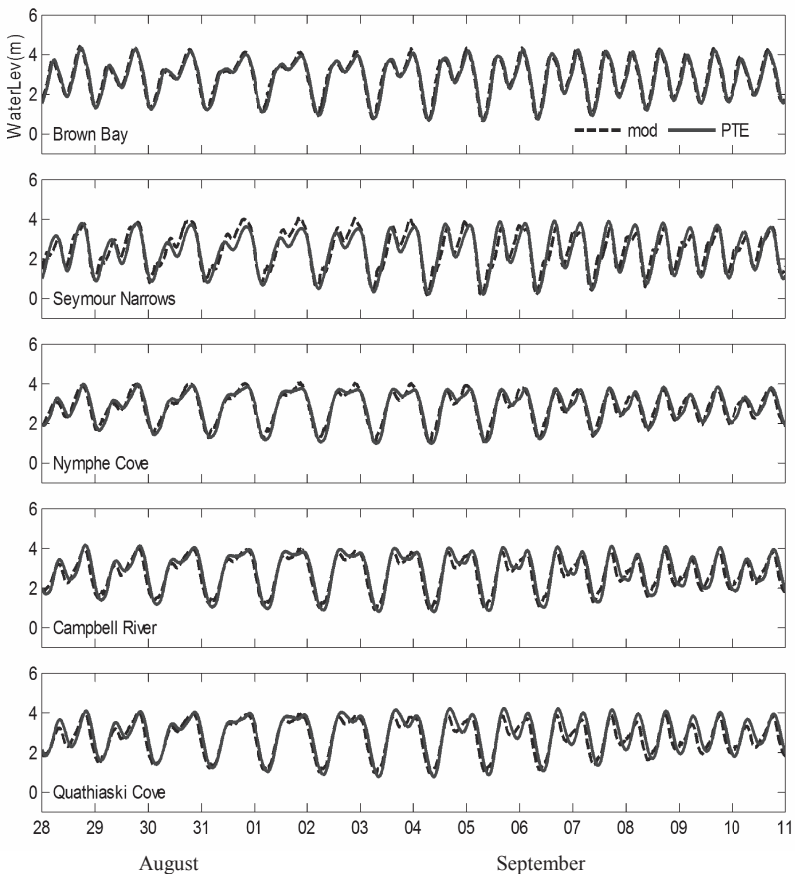


**Figure 6:** Model produced water levels (mod, dashed lines) at the 5 long-term tidal elevation sites as marked in Figure 1, with comparisons to the predicted tidal elevations (PTE, solid lines).

PTE SITE	Brown Bay	Seymour Narrows	Nympe Cove	Campbell River	Quathiaski Cove
RMSD (m)	0.24	0.41	0.26	0.33	0.37

**Table 2:** Root-mean-square deviation (RMSD) between model produced water levels and the predicted tidal elevations (PTE).

The model was also validated by examining the salinity profile crossing Discovery Passage in the vicinity of Campbell River. Three CTD-bottle profile data were achieved outside of Campbell River at around 10:00 AM on Aug28, 1968. The model captured the surface brackish layer that is typically found in estuarine environments (Figure 9). Given the approximate boundary conditions for salinity, model salinities are in reasonable agreement with observations. Overall, the density stratification associated with the river discharge has significant effects on flow near the surface, below 2 – 3 m from the chart datum, and in the vicinity of the river estuary.

#### 4. Roles played by stratification and river discharge

A low salinity plume starting from the Campbell River estuary was found sweeping southward and northward over the channel associated with flood and ebb tides in the baroclinic control run. While the model salinities and temperatures in the barotropic run are time-invariant, model setup and other forcing are the same as in the control run. The difference between the two model runs is generated by the stratification effect and the freshwater discharge from Campbell River. Modeled water levels at the 5 long-term tidal elevation sites (as marked in Figure 1) in the barotropic run are very similar to the model results in the baroclinic control run, therefore they were not shown for comparison here. To focus on the roles played by stratification and river discharge, in this section volume transports and currents from the control run and barotropic run are compared and analyzed.

Scatter plots for volume transport at the southern and northern boundaries through Discovery Passage and the water level difference between the boundaries are shown in Figure 10 based on model results in the control run and barotropic run respectively. The horizontal axis is water level difference at northern and southern open boundaries, which is associated with the hydraulic gradient driving the flow through the channel. Positive water level difference values are associated with northward volume transports. In both control run and barotropic run, volume transports ranged from about  $-2 \times 10^5 \text{ m}^3/\text{s}$  to about  $1.5 \times 10^5 \text{ m}^3/\text{s}$  at the northern boundary, and from about  $-1.2 \times 10^5 \text{ m}^3/\text{s}$  to about  $0.5 \times 10^5 \text{ m}^3/\text{s}$  at the southern boundary. Since northward transports are related to ebb tides and southward transports are related to flood tides, in both model runs flood flows are stronger than ebb flows, which is consistent also with Jiang and Fissel (2007). As it can be seen, the only noticeable difference between the two model runs is that more water is driven

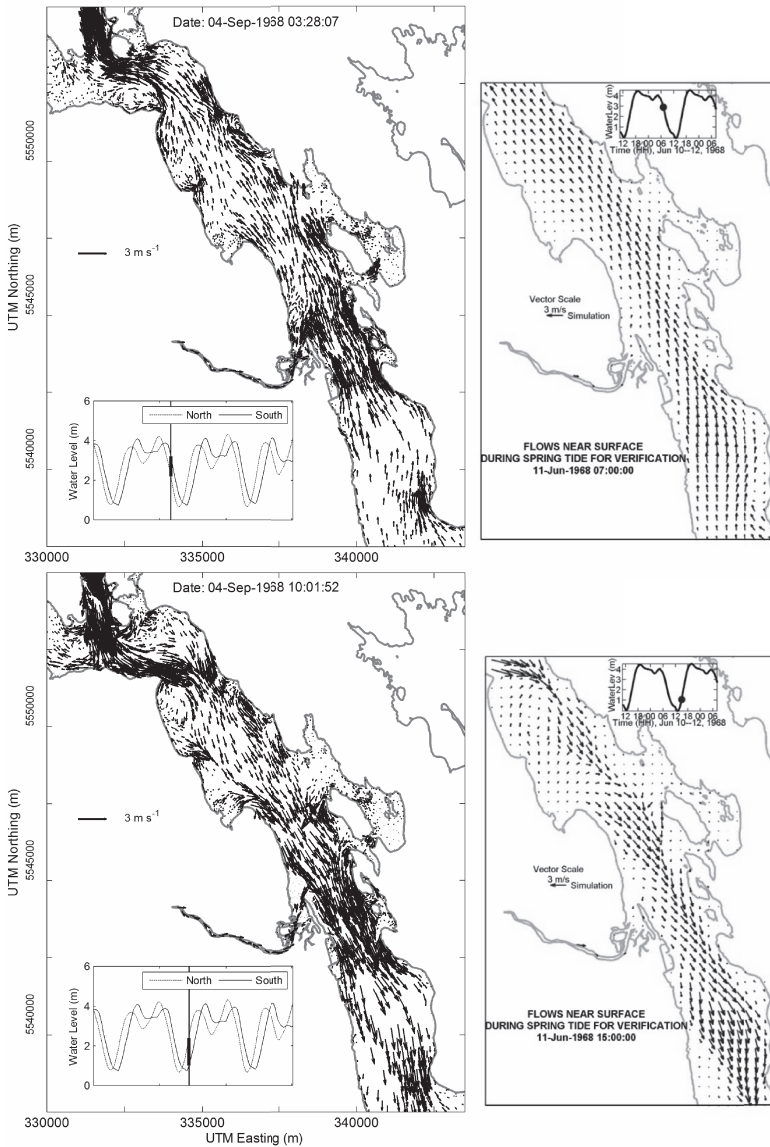


**Figure 7:** Model ebb flows (left and top panel) and flood flows (left and bottom panel) at surface. Velocity arrows are plotted at every 3<sup>rd</sup> element. Right panels are adapted from Jiang and Fissel (2007) for comparison.

into Discovery Passage during flood tides at the northern open boundary in the control run than in the barotropic run.

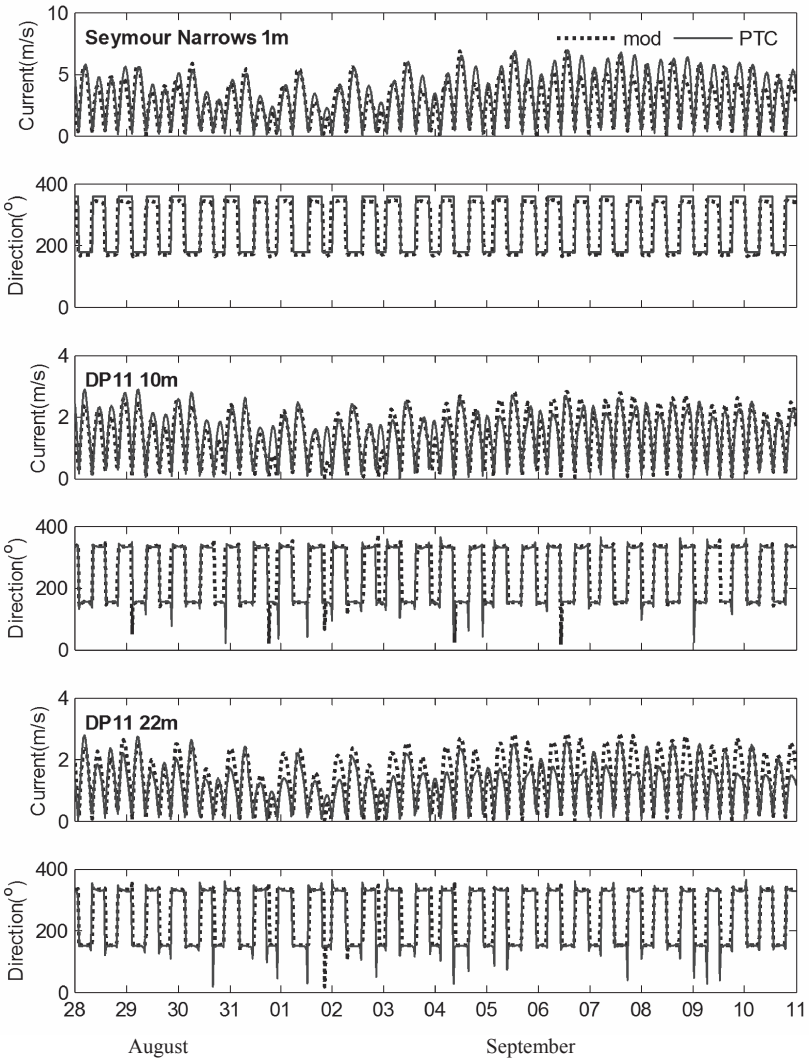


**Figure 8:** Model produced current speeds and directions (mod, dashed lines) at Seymour Narrows (at 1 m depth) and DP11 (at 10 m and 22 m depths separately) as marked in Figure 1, with comparisons to the predicted tidal currents (PTC, solid lines).

PTC SITE	Seymour Narrows (1m)	DP11 (10 m)	DP11 (22m)
RMSD of U (m/s)	0.75	0.19	0.19
RMSD of V (m/s)	0.97	0.38	0.44

**Table 3:** Root-mean-square deviation (RMSD) between model produced and the predicted tidal currents (PTC).

To further examine volume transports at open boundaries affected by stratification and river discharge, the transport differences (transports in the control run minus transports in the barotropic run) at open boundaries were plotted as circles in Figure 11. The scaled radius and grayscale were used to mark the freshwater discharge levels to investigate the influence from Campbell River. At the northern boundary (left panel of Figure 11), the transport difference between the control run and barotropic run is relatively significant, which is up to  $8 \times 10^4 \text{ m}^3/\text{s}$  in amplitude, about 1/3 of the amplitude of total transports through the section. Most differences were recorded in the third quadrant which is associated with flood tides. There was no obvious relationship found between the river discharge and the transport difference in the plot. It then can be argued that the baroclinic effect, which played a role on volume transports in the northern boundary region during the study period, is mainly due to the stratification from initial and open boundary conditions for salinity, rather than due to the freshwater discharge of Campbell River. Meanwhile, as shown in the right panel of Figure 11, transport differences between the control run and the barotropic run at the southern boundary are very small, which indicate that the baroclinic effect is minor in the region of the southern boundary. It should be noted that the role of the boundary condition for inflow salinities, such as the nudging, was not included in the analysis above.

The difference between modeled surface currents (control run – barotropic run) at the current mooring site in Seymour Narrows (as marked in Figure 1) are shown in Figure 12. Relatively large velocity differences (up to  $\sim 2 \text{ m/s}$ ) are found in the eastward components ( $U_{diff}$ ), whose direction is mainly orthogonal to the depth contours based on the bathymetric features in Seymour Narrows. The high frequency variations with a timescale of hours in velocity fields are associated with tidal cycles. The low frequency variations of the envelope of  $U_{diff}$  time series need to be understood. The upper envelope of  $U_{diff}$  is more important since variations of eastward components ( $U$ ) in the control run are larger than in the barotropic run. Modeled salinity fields were examined to find the answer.

Modeled surface salinities at the same site in Seymour Narrows and river discharge from Campbell River (with Y-axis direction reversed) were plotted in the top part of Figure 12 for comparison. Again, high frequency spikes are found in the salinity time series which are caused by tidal cycles. Low frequency variations of the

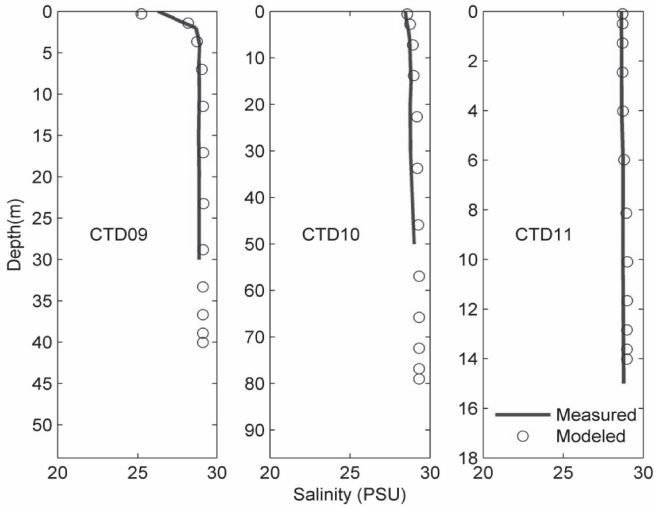


**Figure 9:** Comparisons between modeled and measured salinity at three CTD stations (as marked in Figure 1) at around 10:00 AM on Aug28, 1968.

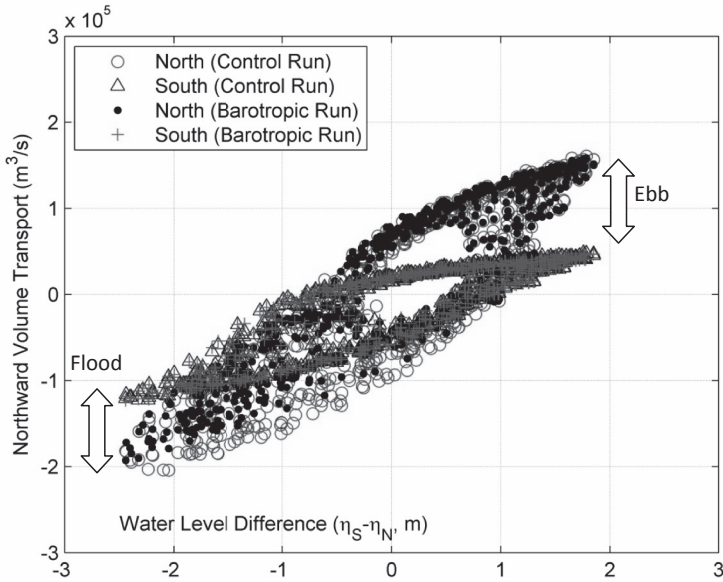


**Figure 10:** Scatter plots for volume transports at the southern and northern boundaries and the water level differences between the two open boundaries from model results during the study period in the control run and barotropic run.

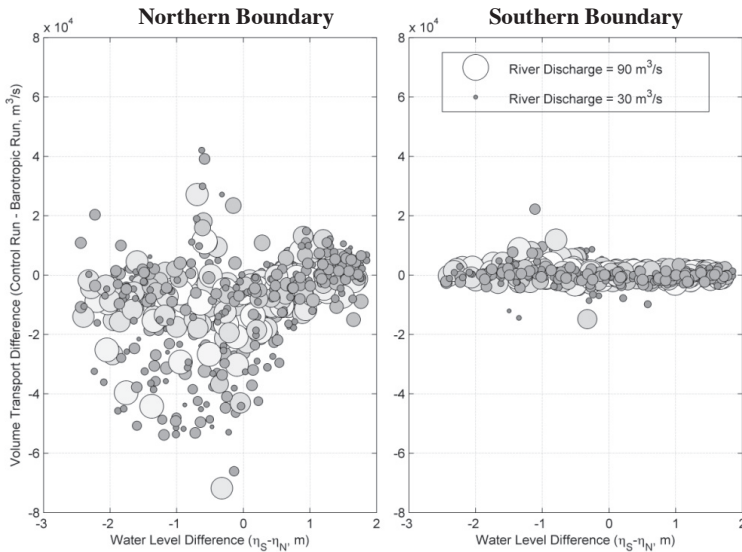


**Figure 11:** Transport differences at each saved output time step (transports in the control run minus transports in the barotropic run) at the northern and southern boundaries during the study period. Associated river discharge records are demonstrated by the radius and grayscale of each circle.

lower envelope of salinity (less salty water) are affected by the river discharge. That is to say the freshwater discharge determined how much low salinity water would be added into the channel and advected to the region in Seymour Narrows during ebb tides. The lower envelope of salinity at Seymour Narrows and the river discharge from Campbell River are correlated to the upper envelope of  $U_{diff}$  time series. Generally the larger  $U_{diff}$  upper envelope coincides with lower salinity lower envelope in Seymour Narrows, caused by the larger freshwater discharge (notice the Y-axis direction of the river discharge reversed in Figure 12). It should be noted that the role played by freshwater discharge from Campbell River during the study period seems to have an influence only on local recirculation flow, rather than on section integrated volume transports, as discussed earlier in this section.

## 5. Summary and conclusion

The unstructured-grid, Finite-Volume Coastal Ocean Model (FVCOM, version 3.1.4) was used for studying the circulation in Discovery Passage (BC, Canada). The model was integrated for 16 days in 1968 with the first 2 days for spin-up process. The model was validated using available historical water surface elevation and ocean current data at different sites, and recent numerical studies. The

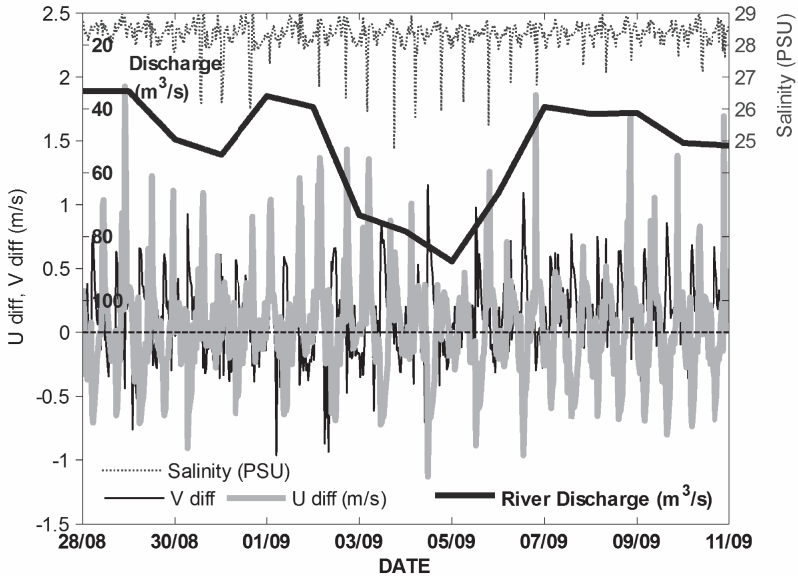


**Figure 12:** Velocity difference at the tidal current site in Seymour Narrows (as marked in Figure 1) between the control run and barotropic run for eastward component (U diff, thick gray line) and northward component (V diff, thin black line). Surface salinity time series (dotted line) and Campbell River discharges (thick black line, with Y-axis direction reversed) during the study period are plotted for comparison.

model produced mean surface current is comparable with the FVCOM model results in Foreman et al. (2012), but captures more details due to much finer horizontal resolution implemented in our model. The model demonstrated a promising capacity for simulating the very strong ocean currents in Seymour Narrows and salinity stratification in the vicinity of Campbell River estuary, as well as resolving the complex geometry.

From comparing model results between the baroclinic control run and a barotropic numerical experiment with uniform and constant salinity and temperature fields, it appears that the vertical stratification was modifying volume transports through the northern open boundary. Freshwater discharge was shown to affect the water salinity in Seymour Narrows, and consequently to drive the current variations crossing the depth contours there. This result indicates the notable influence from stratification and freshwater budget on the mass and tracer flux through the Discovery Passage. Future work will include improving the model by considering more physical processes, such as the surface wind, and carrying on the model study to focus on a

particular area inside the channel such as Canoe Pass located on the eastern side of the southern entrance to Seymour Narrows (Jiang and Fissel, 2007, 2010).

### Acknowledgments

This work was partially funded by the Natural Sciences and Engineering Research Council of Canada (NSERC) Industrial Research and Development Fellowships (IRDF) awarded to Yuehua Lin and ASL Environmental Sciences Inc.

### References

- Canadian Hydrographic Service (CHS). Department of Fisheries and Oceans, Canada. Chart No. 3539 and 3540. Canadian Tide and Current Tables, Vol. 6, Discovery Passage and West Coast of Vancouver Island. <http://www.charts.gc.ca>.
- Institute of Ocean Sciences (IOS)/Ocean Sciences Data Inventory of Rotor Current Meter (RCM) data, Acoustic Doppler Current Meter (ADCP) and S4 current meter data. <http://www.pac.dfo-mpo.gc.ca/science/oceans/data-donnees/index-eng.htm>.
- Hydrometric Database (HYDAT) database. Published by the Water Survey of Canada and available at the following internet address: <http://www.wsc.ec.gc.ca>.
- Chapman, D.C., 1985. "Numerical treatment of cross-shelf open boundaries in a barotropic coastal ocean model." *J. Phys. Oceanogr.*, 15, 1060-1075.
- Chen, C., H. Liu, and R.C. Beardsley, 2003. "An unstructured, finite-volume, three dimensional, primitive equation ocean model: application to coastal ocean and estuaries." *J. Atmos. Oceanic. Technol.*, 20, 159-186.
- Chen, C., R.C. Beardsley, and G. Cowles, 2006a. "An unstructured grid, finite-volume coastal ocean model (FVCOM) system." *Oceanography, Special Issue on "Advances in Computational Oceanography"*. 19(1), 78-89.
- Chen, C., R.C. Beardsley, and G. Cowles, 2006b. "An unstructured grid, finite-volume coastal ocean model: FVCOM user manual." <http://fvcom.smast.umassd.edu>.
- Crean, P.B. and A.B. Ages, 1971. "Oceanographic records from twelve cruises in the Strait of Georgia and Juan De Fuca Strait 1968." Department of Energy, Mines and Resources Marine Sciences Branch, Victoria, Canada.

Fissel, D.B., J. Jiang, R. Birch, J. Buermans, and D. Lemon, 2008. "Assessing the Site Potential for Underwater Turbines in Tidal Channels Using Numerical Modeling and Advanced Ocean Current Measurements." *Proc. IEEE Oceans 2008*, Quebec City, September 2008.

Foreman, M.G.G., 1977. "Manual for Tidal Heights Analysis and Prediction. Pacific Marine Science Report 77-10." Institute of Ocean Sciences, Patricia Bay. Available from anonymous ftp site given on <http://www.pac.dfo-mpo.gc.ca/science/oceans/tidal-marees/index-eng.htm>.

Foreman, M.G.G., D.J. Stucchi, K.A. Garver, D. Tuele, J. Isaac, T. Grime, and M. Guo, 2012. "A Circulation Model for the Discovery Islands, British Columbia." Revised and re-submitted to *Atmosphere-Ocean* January 12, 2012.

Geuzaine, C. and J. Remacle, 2008. "Gmsh: a three-dimensional finite element mesh generator with built-in pre- and post-processing facilities." *Advanced Computational Methods in Engineering (ACOMEN) 2008*, Liège (Belgium), May 26-28, 2008. [abstract]

Jiang, J. and D.B. Fissel, 2007. "3D current modeling in Discovery Passage, British Columbia, for site selection of tidal current turbines." Report for BC Tidal Energy Corporation and Marine Current Turbine Ltd. by ASL Environmental Sciences Inc., Victoria, BC, Canada, 19p. + unnumbered Appendices.

Jiang, J. and D.B. Fissel, 2010. "Applications of 3D Coastal Circulation Numerical Model in Assessing Potential locations of Installing Underwater Turbines." In: *Estuarine and Coastal Modeling: proceedings of the Tenth International Conference*, ed. M.L. Spaulding. American Society of Civil Engineers, 478-493.

Mellor, G. L. and T. Yamada, 1982. "Development of a turbulence closure model for geophysical fluid problem." *Rev. Geophys. Space. Phys.*, 20, 851-875.

Orlanski, I., 1976. "A simple boundary condition for unbounded hyperbolic flows." *J. Comput. Phys.*, 21, 251-269.

Smagorinsky, J., 1963. "General circulation experiments with the primitive equations, I. The basic experiment." *Monthly Weather Review*, 91:99-164.

Sutherland, G., M. Foreman, and C. Garrett. 2007. "Tidal current energy assessment for Johnstone Strait, Vancouver Island." *Proceedings of the Institution of Mechanical Engineers, Part A: Journal of Power and Energy*. 221(2):147-157.